Combined System for Observations of Tropospheric and Stratospheric Thin Clouds

A. ADRIANI, G. P. GOBBI, AND M. VITERBINI

Istituto Fisica dell'Atmosfera, CNR, Frascati, Rome, Italy

S. UGAZIO

Istituto Fisica dello Spazio Interplanetario, CNR, Frascati, Rome, Italy

(Manuscript received 17 September 1991, in final form 23 March 1992)

ABSTRACT

A balloonborne sonde and a polarization lidar have been developed to make combined observations of thin tropospheric and stratospheric clouds. In their first application these instruments have been used in a campaign organized to study Antarctic polar stratospheric clouds (PSCs), which are deeply involved in the process of ozone depletion.

The sonde collects cloud particles larger than 4 μm in diameter on a transparent impactor and observes them by means of a CCD (charge coupled device) camera microscope. Images are transmitted in real time to the ground station for recording and analysis. Shape, dimension, and size distribution of the particles are obtained from these frames. The lidar provides complementary information about the cloud optical depth, backscattering, depolarization, vertical distribution, and temporal evolution.

Characteristics of both instruments are described. The experiments performed during the 1990 spring campaign at McMurdo Station, Antarctica, are discussed, and some results are reported to show the capabilities of the combined system.

1. Introduction

The presence of optically thin stratospheric clouds over Antarctica has been observed by satellite (McCormick et al. 1982; McCormick and Trepte 1986), lidar (Iwasaka 1986), and in situ observations (Hofmann et al. 1989; Hofmann and Deshler 1991). Formation of these polar stratospheric clouds (PSCs) is triggered by the very low temperatures reached by the stratosphere during the Antarctic winter and spring. Mostly residing between 10 and 25 km in altitude, PSCs show a typical vertical extent of 1–2 km, while, in the horizontal, they can span hundreds of kilometers. In recent years it became evident that PSCs play an important role in the depletion of polar ozone (Toon et al. 1989; Solomon 1990). PSCs are composed of a nitric acid trihydrate (NAT) solution (Hanson and Mauersberger 1988). This is because in the stratosphere, NAT condensation temperature is 4–5 K higher than the water frost point. As indicated by measurements (Deshler et al. 1991; Hofmann and Deshler 1991), PSCs in the Antarctic stratosphere are often characterized by a bimodal size distribution, with most of the mass contained in the second mode (mode radius 2–3 μm). Large particles can grow in two different cases: 1) when the temperature reaches the water frost point, approximately 190 K (PSC type II), and 2) when pure NAT clouds (PSC type I) nucleate selectively on a few particles only. Due to the larger water abundances, particles formed in case 1 can reach larger sizes than in case 2.

One of the uncertainties associated with PSC studies is the lack of knowledge of the microphysical and chemical properties of their particles. This is particularly true in the fast-settling sizes ranging beyond 2-μm diameters. Due both to their low number concentration and irregular shape, this class of particles is difficult to measure and, consequently, poorly known. Yet, parameters such as size distribution, concentration, and morphology are important in understanding and modeling the chemical–physical processes in which PSCs are involved.

In this paper, the experiment BACI [balloonborne aerosol CCD (charge coupled device) imaging] will be described. This experiment was designed to measure characteristics of large particles in PSCs and cirruslike clouds. The first observations were aimed at the study of PSCs in Antarctica for the purpose of determining their contribution to denitrification, dehydration, and the development of heterogeneous chemical reactions in the polar stratosphere. The experiment was operated at the end of the 1990 polar night at the U.S. station at McMurdo (78°S, 167°E). Results from this campaign will also be presented.

Corresponding author address: Dr. Alberto Adriani, Instituto di Fisca dell'Atmosfera, Consiglio Nazionale delle Ricerche, Via G. Galilei, CP 27, 00044 Frascati, Italy.

© 1993 American Meteorological Society

Unauthenticated | Downloaded 05/19/25 05:18 AM UTC

2. Instrumentation

BACI is a sounding system developed for in situ observations of cloud crystals larger than 4 μm in diameter. Ground support is supplied by a small lidar designed for stratospheric cloud observations. The lidar reveals the presence of PSCs before launch of the sonde and provides information about vertical extent, optical depth, and optical depolarization properties of the cloud itself. A Vaisala sonde included in the balloon payload provides measurements of temperature, pressure, humidity, wind direction, and wind strength.

a. Balloonborne sonde

The technical features of BACI are reported in Table 1, and a block diagram of the sounding system is given in Fig. 1. The sonde has a microscope objective mounted on a CCD videocamera. The CCD microscope system observes the cloud particles across a sapphire impactor placed in front of the objective. The impactor is housed in a chamber where air from the outside environment is aspirated through a nozzle (dimensions in Fig. 2). The impactor observing area is on the nozzle axis and has a size of 550×412 μm^2.

The airflow is generated by means of a centrifugal turbine and is maintained in a laminar regime to provide inertial capture of the ice crystals on the surface of the impactor (Ranz and Wong 1952; Prodi et al. 1981). Experimental tests have been performed to identify the best fluid-dynamics solution for the structure of the impactor, the nozzle, and the centrifugal turbine. Preliminary tests have been performed by means of a Hele-show (streamline-visualization technique), using a bidimensional simulation of the model. Then a full-size model, reproducing the final geometry, was tested using laser Doppler anemometer (LDA) techniques. To determine the system-capturing performance, as well as to estimate the concentration of particles collected during the experiment, requires knowledge of the air flux through the nozzle, which can be calculated from the airspeed. Assuming that the air is a perfect gas, and the flow in the nozzle is isentropic, an average value of the airspeed can be computed by the formula (Sabersky et al. 1989)

$$v^2 = 2c_pT\left[1 - \left(\frac{p_n}{p_e}\right)^{(\gamma-1)/\gamma}\right], \qquad (1)$$

where p_n and p_e are, respectively, the pressure at the end of the nozzle and in the outside environment, T the air temperature, $\gamma = c_p/c_v$, and c_p and c_v the air specific heats. In a laminar regime, the airspeed is maximum on the nozzle axis and $v_a = 2v$. Since the impactor observing area is placed on the nozzle axis and its size is about one-tenth of the nozzle diameter, v_a has been used for computing the impaction parameters ahead. Air flux is computed across a cross section equal to the observing area. Assuming that the air volume the centrifugal pump can remove from the impactor chamber is only a function of its rotation speed, that is, volume losses can be neglected, it can be demonstrated, using (1), that the flux through the nozzle is independent of the external environment. Thus, after calibration in a controlled environment, the air flux can be retrieved by measuring only the rotation speed of the turbine. To confirm this hypothesis, calibration tests were performed in a thermobaric chamber. Pressure inside the nozzle was measured for different environmental pressures and turbine speeds. The airspeed was then calculated from (1) and plotted against pump speed in Fig. 3. The resulting empirical law relating the flux rate to the centrifugal pump rotation is shown in Fig. 4. The relationship was derived from the best linear fit to all the airspeed values obtained from (1), using the measured p_n/p_e ratios at various environmental pressures and at different pump speeds (Fig. 3). As shown in Fig. 3 there is a slight dependence of p_n/p_e on external pressure; however, the law described in Fig. 4 is a good approximation of the actual behavior of the system in the 200–50-mb pressure range, and the linear fit is well within the measurement errors. The calculated Reynolds number N_{Re} ranges between 400 and 1200, granting a laminar regime in the nozzle.

Laboratory tests performed on the full-size model were aimed at verifying the behavior of the air flux in the volume facing the impactor. A second goal was to check if the application of the Ranz and Wong theory to the model provided a good description of the instrument performance. During the lab tests, the sucked air was seeded with particles ranging between 1 and 120 μm. The analysis of many pictures of the air flux highlighted by the particles in the proximity of the impactor testified to the correct performance of the system, according with the hypothesis. Accurate tests were performed in the airspeed range between 100 and 200 m s^{-1}. Agreement of the LDA results with the values calculated by differential pressure measurements was good. The linear dependence of the airspeed on the turbine velocity suggested a good extrapolation of the calculation at lower values as given in Figs. 3 and 4. In fact, successive laboratory tests recommended that the velocity of the air at the nozzle exit must be kept low enough to avoid possible breaking of complex crystals. Breaking was observed on large crystals for air fluxes larger than 10 cm^3 s^{-1} (airspeed about 40 m s^{-1}). The crystals shown in Fig. 5 were collected

TABLE 1. BACI technical data.

Microscope	16×, resolution 1 μm
Videocamera	SAFO TH63DVC, CCD Thomson, CCIR, 576 × 384 pixels (8.8 mm × 6.6 mm)
Telemetry	231 MHz, BW 5 MHz, 10 W for images transmission, 160 MHz for remote controls
Image processing	Data translation DT2858, DT2851 on Epson AX, CPU 80286 (8/12 MHz)

Unauthenticated | Downloaded 05/19/25 05:18 AM UTC

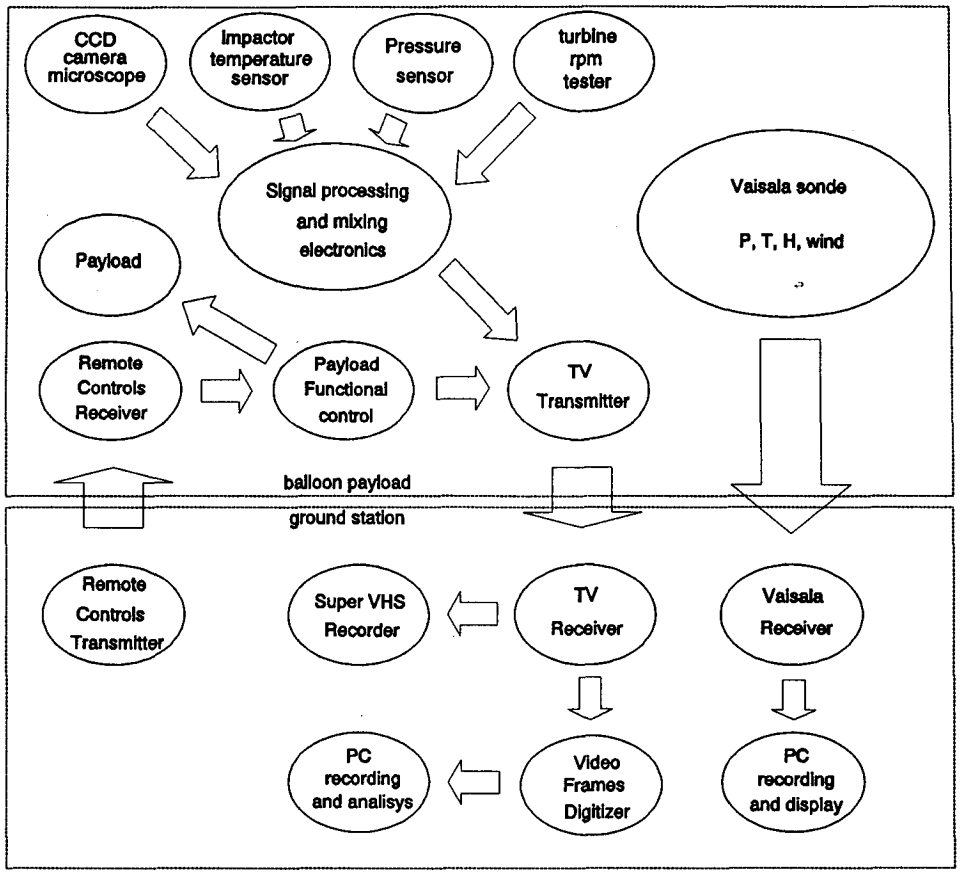

FIG. 1. BACI block diagram.

during a laboratory test with flows of 10 $cm^3 s^{-1}$ and were formed in a cloud chamber at −18°C. The smaller crystals have diameters of 4–5 μm.

The volume flux rates during two different flights performed in Antarctica in 1990 are shown in Fig. 6. At altitudes where cirrus clouds or PSCs can be observed, the air volume flux rate ranged between 5 and 7 $cm^3 s^{-1}$. Turbine speeds were continuously monitored during the flight. Variations of the flux rate as a function of altitudes were due to the decreasing air density, which means a smaller resistance of the air to the engine motion, and to the influence of colder temperatures on the mechanics and power supply. Inside PSCs, particle concentration as low as 10^{-3} cm^{-3} is expected. In the cirrus clouds, concentrations can be an order of magnitude higher or more, so the time necessary to collect at least one particle can vary from a few tenths of seconds to a few minutes.

According to the geometry of the BACI impactor, the models used by Ranz and Wong (1952) for impaction of a round jet of defined diameter on a flat plate of infinite extent are appropriate to calculate the collection efficiency of the impactor chamber. The results indicate that, for particles with diameters larger than 4 μm, the efficiency is larger than 90%. This assumes the density of the ice crystals to be 0.9 g cm^{-3} (Pruppacher and Klett 1980), and that the Cunningham slip-correction factor for resistance of a gas to movement by small particles is approximately 1.

In flight the impactor is periodically heated to evaporate the ice crystals. Once heating is stopped, the airflow rapidly restores the initial temperature condition. A temperature microsensor is placed very close to the

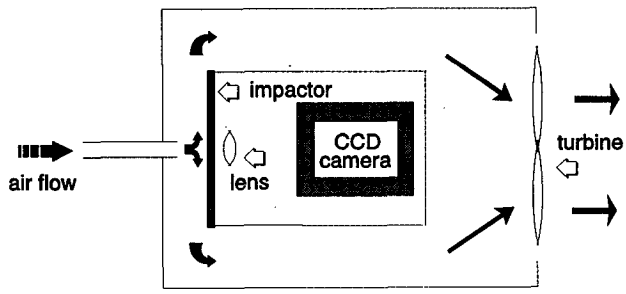

FIG. 2. BACI impaction chamber. The diameter of the nozzle is 5 mm, impactor diameter is 50 mm, and distance nozzle impactor is 14 mm.

Unauthenticated | Downloaded 05/19/25 05:18 AM UTC

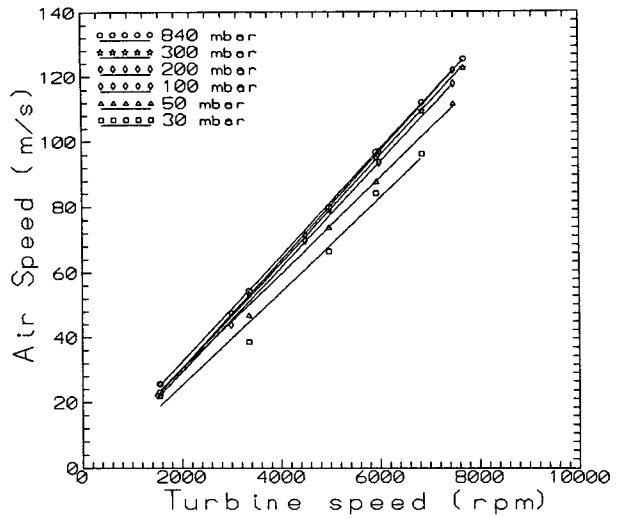

FIG. 3. Calculated airspeed in the nozzle from the ratio p_n/p_e. Each line represents the best fit to the values taken at different p_e as given in the legend.

central observation area, both to discriminate against crystals captured at temperatures different from those of the external environment, and to control the defrosting cycle. Experience revealed that self-cleansing of the impactor often occurs after impaction. In fact, if the particle concentration and air humidity are not too high, the airflow itself is sufficient to evaporate the ice crystals. This behavior was noticed during all the 1990 flights from McMurdo.

The image of the impactor central area is magnified 16 times by means of a flat-field microscope objective focusing on a black and white, CCD videocamera, with resolution better than 500 TV lines. Information from three sensors placed on the sonde are included as bars in the video signal before it is transmitted to the ground station. These sensors measure the impactor temperature, the environment pressure, and the turbine speed. The signal is sent to the ground station by standard CCIR video transmission at 231 MHz, the bandwidth is 5 MHz, and the carrier microwave is AM neg-modulated. The TV signal received at the ground station is continuously stored on two super-VHS tape recorders. Personal computer–installed data translation cards DT2851 and DT2858 are used for off-line digitization and processing of the data. Real-time elaboration and storage of the images may be performed by means of the same cards. The sonde is also equipped with a 160-MHz receiver. Eight different commands can be sent from the ground to control such functions of the sonde as payload–balloon separation, automatic or manual impactor defrosting, and on–off switching of the transmitter. The transmitter is automatically turned off at landing. After a programmed lapse of time from landing, a digital timer switches on the TV transmitter. The instrument then acts as a beacon, indicating its position for recovery. The payload weight is 19 kg and, in the polar stratosphere, a 750-m^3 helium balloon can lift it to heights of approximately 23 km. A Vaisala sonde is flown with the payload to get measurements of meteorological parameters. These are sent to the ground station via a separate 400-MHz, FM channel. The Omega system of the Vaisala sonde provides the wind field and the position of the payload during ascent. An estimated landing point for recovery can then be calculated.

b. Lidar

The lidar developed for the experiment is based on an Nd-YAG laser emitting 140 mJ at 532 nm, and on a 41-cm Newtonian telescope. Daytime operation is allowed by a narrow telescope field of view of 0.6 mrad, and a 0.15-nm bandwidth interferential filter. Perpendicular polarizations of the backscattered light (parallel and orthogonal to the laser polarization) are separated by a cube polarizer and detected by two photomultipliers. The output signals are digitized at 100 MHz by a two-channel, averaging digital oscilloscope, and stored on a PC. The instrument vertical resolution is 3 m, but height averages are performed to increase the signal-to-noise ratio. Maximum height reached by the system is approximately 26 km. At this level the signal amplitude is approximately three times the standard deviation of the nighttime background noise. Daytime operation reduces the maximum range down to approximately 20 km.

The primary information from the lidar is the backscattering ratio R:

$$R = \frac{\beta_a + \beta_m}{\beta_m}, \tag{2}$$

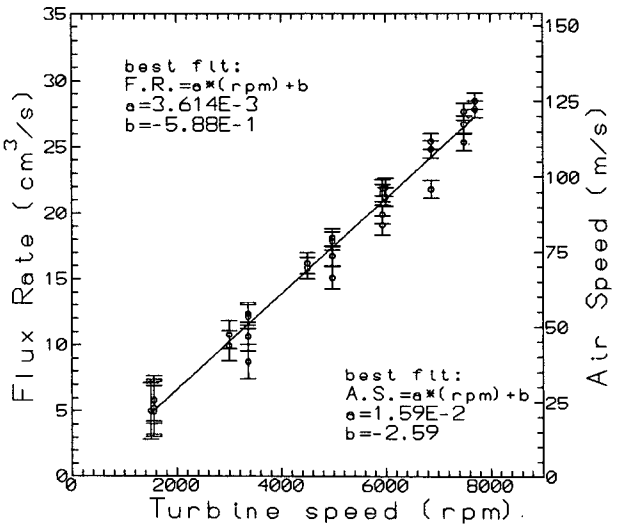

FIG. 4. Flux-rate calibration curve. The two best fits permit us to calculate, respectively, the air flux rate (FR) and airspeed (AS) from the measured turbine speed.

Unauthenticated | Downloaded 05/19/25 05:18 AM UTC

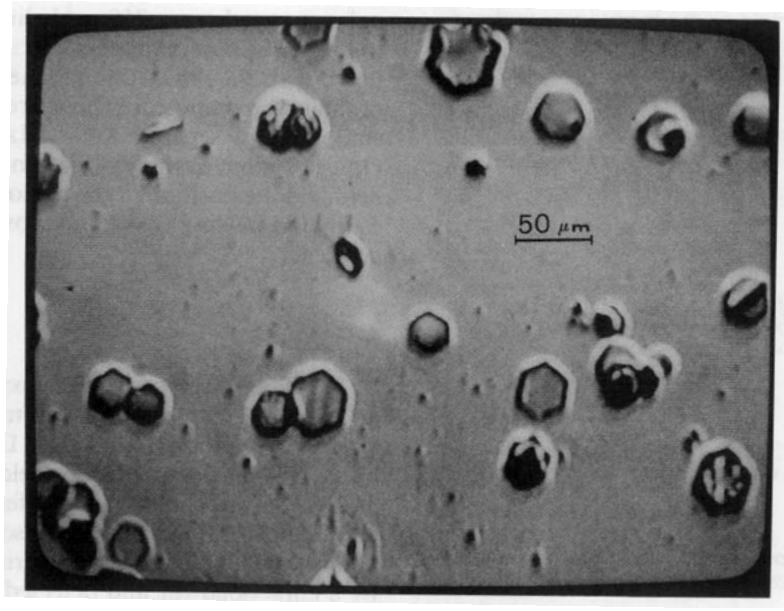

FIG. 5. TV image of ice crystals collected during BACI laboratory tests.

where β_a and β_m are, respectively, the aerosol and molecular backscattering cross sections. The term $\beta_a + \beta_m$ is proportional to the lidar signal times the squared distance from the ground. Molecular backscattering is calculated from the atmospheric number density by means of temperature and pressure sounding. A backscattering ratio $R = 1$ represents an aerosol- and cloud-free atmosphere. Higher values indicate the amount of backscattering due to aerosols or clouds. In order to estimate the scattering ratio, the lidar signal has to be calibrated. Calibration is performed, making it equal to the calculated molecular signal where the atmosphere is particle-free. Calibration heights are usually chosen above 23 km, where the aerosol contribution is commonly negligible (Deshler et al. 1991).

3. Discussion of results

The combined system BACI and lidar was employed for the first time at McMurdo Station, Antarctica, during the development of the severe 1990 ozone hole. More than 60 lidar measurements were taken during the period; these are discussed by Gobbi et al. (1991) and Deshler et al. (1991). Unfortunately, since the beginning of September the stratospheric temperature never reached values low enough for the formation of large PSC crystals. Only a few PSCs were present over the station during the campaign. According to other measurements performed at the same site (Deshler et al. 1991), when PSCs were observed, their particles never ranged beyond 4 μm in diameter. Two launches were conducted when stratospheric temperatures were as low as −79°C. No evidence for large particles in PSCs was observed. The flight of 7 October 1991 was performed to observe a type I PSC and stratified, optically thin clouds. Cirrus cloud particles are expected to be in the same size range as type II PSC. One of the frames received from BACI during this flight is depicted in Fig. 7. The high noise on the image was given by the unfavorable position of the dipole antenna with respect to the receiving station. In this frame only the encircled particle was collected in the lower cloud around 5.5 km; the others are solid background particles collected during the launching phase. The cirrus particle is approximately 20 μm in diameter.

The results of the combined experiment are synthesized in Fig. 8. Data are from both lidar and balloonsonde. The lidar-depolarization ratio is reported in curve (a), while the backscattering ratio (as $R - 1$) is

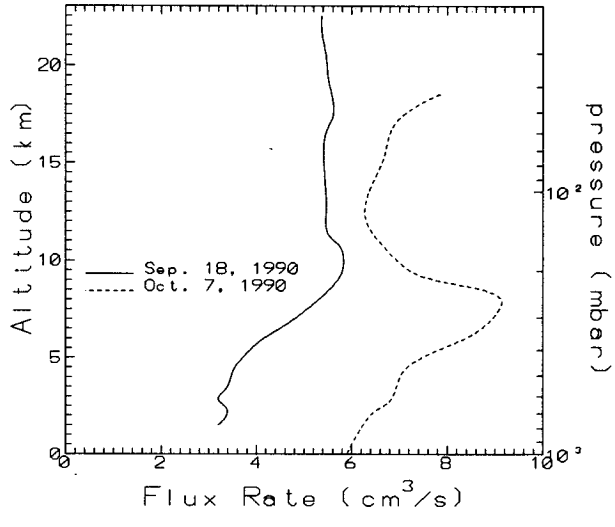

FIG. 6. Sampled air volume during two different flights.

Unauthenticated | Downloaded 05/19/25 05:18 AM UTC

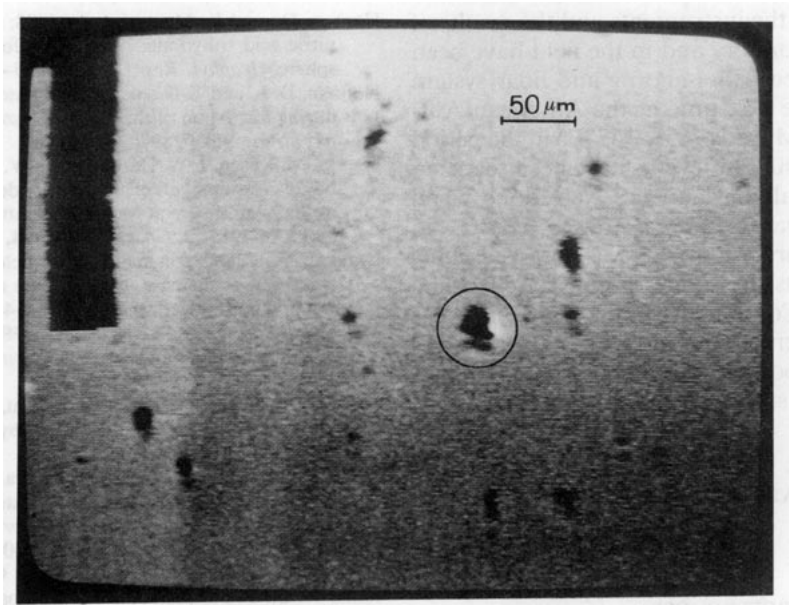

FIG. 7. Example of particle image transmitted during the 7 October 1990 flight.

given in curve (b). The depolarization ratio is calculated as the ratio between depolarized and nondepolarized signal. Since spherical particles do not depolarize, depolarization is a good indicator of asphericity, that is, a change from droplet to crystal, of the cloud particles. It is impossible, however, to give a quantitative evaluation about depolarization using only one wavelength. Comparison of curves (a) and (b) indicates that the higher part of the cirrus cloud (about 10 km), and the stratospheric cloud around 12 km, are mainly composed of small spherical particles. According to the lidar trace, the clouds extended between 4.8 and 10.4 km, which is the tropopause level, as shown by the temperature profile in curve (c). Large particles were collected only in the lower cloud region, between the horizontal lines (5.2–5.7 km). At this level the balloon ascent velocity was 4.3 m s^{-1}. Measured concentration of particles larger than 4 μm was 7.4 $\times 10^{-3}$ cm^{-3}. The particles exhibited irregular shapes as shown in Fig. 7, while sizes ranged between 5 and 25 μm. Such shape is consistent with the high values of depolarization observed at these levels. Temperature and relative humidity were obtained by the Vaisala meteosonde. Relative humidity is corrected for ice saturation pressure. Comparison of the relative humidity and lidar profile with BACI images suggests either that the upper layers of the cloud were not present in the area where the balloon ascended, or that, at higher levels, the cloud was mainly composed of smaller particles not observable by BACI. The relative humidity profile also indicates that the cirrus particles were not in thermodynamic equilibrium, probably evaporating. In fact, a dissipating patched-cloud spatial distribution was visually observed during the experiment, particularly in the higher troposphere.

4. Conclusions

An experiment for the study of optically thin clouds by means of balloonborne sonde and lidar has been presented. The sonde has been primarily designed to study clouds where particle concentrations can be as low as 10^{-3} cm^{-3}, as can be observed in cirrus clouds and PSCs. The lidar is sensitive to all aerosols and PSCs in the lower stratosphere.

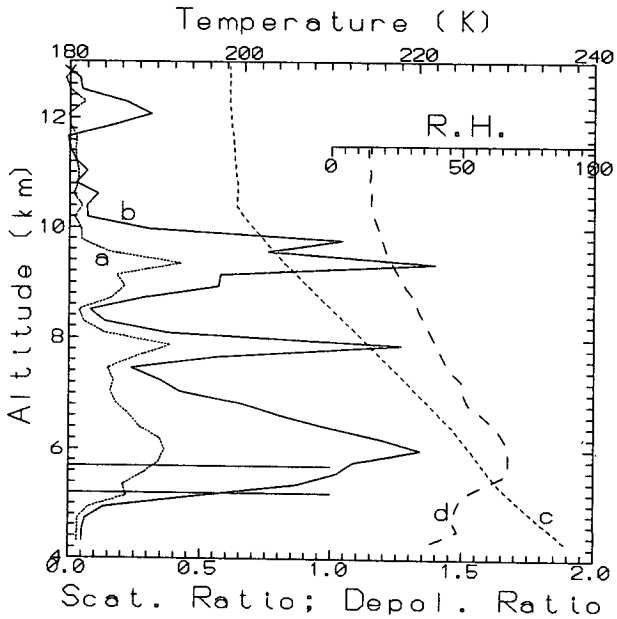

FIG. 8. Measurements on 7 October 1990: (a) lidar depolarization ratio, (b) lidar scattering ratio as $R - 1$, (c) air temperature, and (d) relative humidity.

Unauthenticated | Downloaded 05/19/25 05:18 AM UTC

Characteristics of the instruments and the results of tests both in the laboratory and in the field have been given. This combined balloonborne and lidar system was operated for the first time at the American Antarctic Station of McMurdo (78°S, 167°E) in the period August–October 1990. PSC events have been scarce in that season. Two balloon launches were done when stratospheric temperatures were as low as −79°C. No evidence for large particles in PSC was observed. During one of the flights the sonde sampled a cirruslike cloud and a PSC. Combined results from this measurement were presented and indicate both the feasibility of the balloonborne experiment, and advantages of the system in the study of thin, frozen clouds.

Acknowledgments. This project is supported by the Italian Program for Antarctic Research (PNRA) under Grant FAADR.

REFERENCES

Deshler, T., A. Adriani, D. J. Hofmann, and G. P. Gobbi, 1991: Evidence for denitrification in the 1990 Antarctic spring stratosphere: II aerosols. *Geophys. Res. Lett.*, **18,** 1999–2002.

Gobbi, G. P., T. Deshler, A. Adriani, and D. J. Hofmann, 1991: Evidence for denitrification in the 1990 Antarctic spring stratosphere. I: Lidar and temperature measurements. *Geophys. Res. Lett.*, **18,** 1995–1998.

Hanson, D., and K. Mauersberger, 1988: Laboratory studies of the nitric acid trihydrate: Implication for the South Polar stratosphere. *Geophys. Res. Lett.*, **15,** 855–858.

Hofman, D. J., and T. Deshler, 1991: Stratospheric cloud observation during formation of the Antarctic ozone hole in 1989. *J. Geophys. Res.*, **96D,** 2897–2912.

——, J. M. Rosen, J. W. Harder, and J. V. Hereford, 1989: Balloonborne measurements of aerosols, condensation nuclei, and clouds in the stratosphere at McMurdo Station Antarctica, during the spring of 1987. *J. Geophys. Res.*, **94,** 11 253–11 269.

Iwasaka, Y., 1986: Non-spherical particles in the Antarctic polar stratosphere, increase in particulate content and stratospheric water vapor budget. *Tellus,* **38B,** 364–374.

McCormick, M. P., and C. R. Trepte, 1986: SAM II measurements of Antarctic PSCs and aerosols. *Geophys. Res. Lett.*, **13,** 1276–1279.

——, H. M. Steele, P. Hamill, W. P. Chu, and T. J. Swissler, 1982: Polar stratospheric cloud sightings by SAM II. *J. Atmos. Sci.*, **39,** 1387–1397.

Prodi, F., M. Caporaloni, G. Santachiara, and F. Tampieri, 1981: Inertial capture of particles by obstacles in form of disks and stellar crystals. *Quart. J. Roy. Meteor. Soc.*, **107,** 699–710.

Pruppacher, H. R., and J. D. Klett, 1980: *Microphysics of Clouds and Precipitation.* Reidel Publishing Co., 41 pp.

Ranz, W. E., and J. B. Wong, 1952: Impaction of dust and smoke particles. *Ind. Eng. Chem.*, **44,** 1371–1381.

Sabersky, R. H., A. J. Acosta, and E. G. Hauptmann, 1989: *Fluid Flow: A first course in fluid mechanics.* Macmillan Publishing Co., 301–315.

Solomon, S., 1990: Progress towards a quantitative understanding of Antarctic ozone depletion. *Nature,* **347,** 347–354.

Toon, O. B., R. P. Turco, J. Jordan, J. Goodman, and G. Ferry, 1989: Physical processes in polar stratospheric ice clouds. *J. Geophys. Res.*, **94,** 11 359–11 380.

Unauthenticated | Downloaded 05/19/25 05:18 AM UTC